

STUDYING THE AERODYNAMICS OF APPARATUS WITH
A NONMOVING GRANULAR BED

Sh. A. Ershin, U. K. Zhapbasbaev, M. Sh. Kulymbaeva,
and L. G. Khadieva

UDC 532.546

A displacement reactor with a nonmoving granular bed (NGB) and equipment in which radial influx follows Z- and II-shaped flow patterns have found widespread application in technological processes. In connection with the fact that the distribution of the mixture reacting within the granular bed is governed by the overall aerodynamic situation within the equipment, an exact solution for the problem demands consideration of corresponding systems of equations of motion in the free parts of the equipment and within the NGB. Hydrodynamic models of such reactors, based on the theory of an ideal fluid [1-3], are based on the joint consideration of a system of Euler equations with a linear or nonlinear Darcy law. The calculation is constructed separately in each region, with satisfaction of the conditions of conjugacy at the boundaries separating the media, and it makes it possible to determine the velocity and pressure fields for a given distribution of vorticity at the inlet section [2]. As demonstrated by experiments, in the free sections of equipment with NGB we encounter separation phenomena and stagnation zones [4], which are not described within the framework of the ideal-fluid model. These phenomena influence the distribution of the flow in the NGB and can be explained by proceeding from the theory of a viscous fluid. The model of a viscous fluid in porous media has been dealt with in numerous studies. In particular, a study was undertaken in [5] on the motion of a viscous fluid in a tube with a granulated filler, and an explanation is provided for the appearance of macroscopic nonuniformities in the velocity profiles, attributable to the rise in the porosity of the bed near the wall. However, no calculations were carried out for equipment with NGB. We present some of the results below from an investigation into the aerodynamics of reactors with NGB, based on the theory of a viscous fluid.

1. Formulation of the Problem. We examine a steady plane flow of a viscous incompressible fluid in equipment with NGB. The regions of flow in front of and behind the granular bed are identified with G_1 and G_3 , and inside the granular bed they are identified as G_2 (Fig. 1). If we use the method of averaging over the fluid phase for the local volume of the porous medium [6, 7], then the system of equations of motion and continuity can be written in unified form, valid for all flow regions G_i :

$$u \frac{\partial u}{\partial x} + v \frac{\partial u}{\partial y} = -\frac{\partial p}{\partial x} + \frac{h}{\text{Re}} \left[2 \frac{\partial^2 u}{\partial x^2} + \frac{\partial}{\partial y} \left(\frac{\partial v}{\partial x} + \frac{\partial u}{\partial y} \right) \right] - \zeta u; \quad (1.1)$$

$$u \frac{\partial v}{\partial x} + v \frac{\partial v}{\partial y} = -\frac{\partial p}{\partial y} + \frac{h}{\text{Re}} \left[2 \frac{\partial^2 v}{\partial y^2} + \frac{\partial}{\partial x} \left(\frac{\partial v}{\partial x} + \frac{\partial u}{\partial y} \right) \right] - \zeta v; \quad (1.2)$$

$$\partial \epsilon u / \partial x + \partial \epsilon v / \partial y = 0, \quad (1.3)$$

where ϵ is the porosity of the bed; $\zeta = 150(1 - \epsilon)^2 DL / (\epsilon^2 d_3^2 \text{Re})$; $h = D/L$; $\text{Re} = u_0 D / \nu$; D represents half the height of the inlet section and L is a characteristic dimension.

In regions G_1 and G_3 ($\epsilon = 1$) system (1.1)-(1.3) represent the Navier-Stokes equations, while in G_2 ($\epsilon < 1$) it describes the motion of a viscous fluid in an isotropic porous medium. Neglecting the inertial terms in (1.1)-(1.3) for G_2 leads to the Brinkman model [8], while if we neglect the viscosity terms we come up with the dynamic model [9].

System (1.1)-(1.3) is solved under the following boundary conditions:

Alma Ata. Translated from Zhurnal Prikladnoi Mekhaniki i Tekhnicheskoi Fiziki, No. 4, pp. 128-133, July-August, 1990. Original article submitted February 22, 1988; revision submitted February 15, 1989.

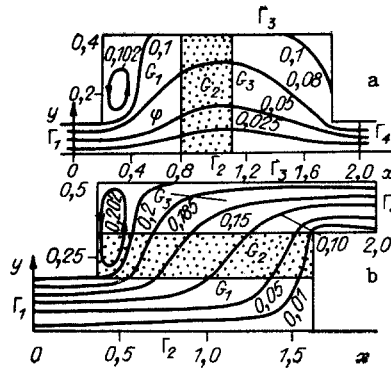


Fig. 1

$$\begin{aligned}
 \Gamma_1: u &= \varphi_0(y), v = 0; \\
 \Gamma_2: \partial u / \partial y &= 0, v = 0; \\
 \Gamma_3: u &= 0, v = 0; \\
 \Gamma_4: \partial u / \partial x &= 0, v = 0, p = p_0
 \end{aligned}
 \tag{1.4}$$

(p_0 is the constant pressure which is referred to the regime parameters).

A parabolic or rod-shaped profile for the longitudinal component of velocity was established at the inlet to the apparatus. The possibility of formulating the conditions of adhesion in the Brinkman model has been demonstrated rather convincingly in the experimental studies covered in [10]. The condition of adhesion is therefore utilized on Γ_3 .

System (1.1)-(1.3) was solved by a numerical method with the aid of the algorithm proposed [11]. For this purpose we will bring system (1.1), (1.2) to the form

$$\frac{\partial}{\partial x} \left(H - \frac{2h}{\text{Re}} \frac{\partial u}{\partial x} \right) = v\omega + \frac{h}{\text{Re}} \frac{\partial \tau}{\partial y} - \zeta u;
 \tag{1.5}$$

$$\frac{\partial}{\partial y} \left(H - \frac{2h}{\text{Re}} \frac{\partial v}{\partial y} \right) = -u\omega + \frac{h}{\text{Re}} \frac{\partial \tau}{\partial x} - \zeta v
 \tag{1.6}$$

In standard fashion [12] we will then use (1.3), (1.5), (1.6) to find the conditions

$$\left(H - \frac{2h}{\text{Re}} \frac{\partial u}{\partial x} \right)_- = \left(H - \frac{2h}{\text{Re}} \frac{\partial u}{\partial x} \right)_+, \quad \tau_- = \tau_+, \quad (\varepsilon u)_- = (\varepsilon u)_+, \quad v_- = v_+.
 \tag{1.7}$$

The subscripts - and + pertain, respectively, to the flow parameters in front of and behind the separation surface. In the case of an ideal-fluid model, Eqs. (1.7) coincide with the conditions from [9].

Direct calculation of system (1.1)-(1.3) is accomplished by taking into consideration the satisfaction of (1.7) on transition through the separation boundary G_1 .

Using the condition of single-valuedness for the calculation of the total pressure H over the elementary contour $\oint_C \nabla H ds = 0$ and the finite-difference analogies (1.5), (1.6),

we can derive the finite-difference equation for the determination of the vorticity ω . In approximation of the convective terms relative to ω we use the "counterflow" differences of the second kind [13], while in approximation of the diffusion and source terms we use the recommendations from [14].

The stream function ψ is introduced through the equalities $\partial \psi / \partial y = u\varepsilon$, $\partial \psi / \partial x = -v\varepsilon$ and is found from the equation

$$\frac{\partial}{\partial x} \left(\frac{1}{\varepsilon} \frac{\partial \psi}{\partial x} \right) + \frac{\partial}{\partial y} \left(\frac{1}{\varepsilon} \frac{\partial \psi}{\partial y} \right) + \omega = 0.$$

The boundary conditions ω , ψ are set in accordance with (1.4). The vorticity value at the wall is calculated by means of the Thom formula in conjunction with the method of lower relaxation.

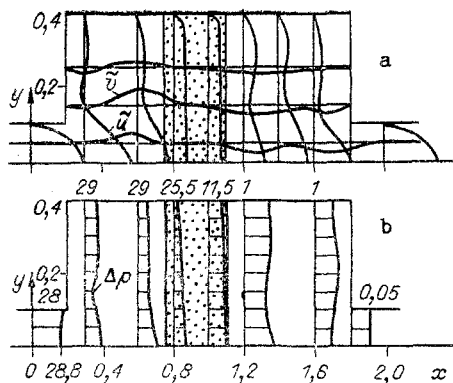


Fig. 2

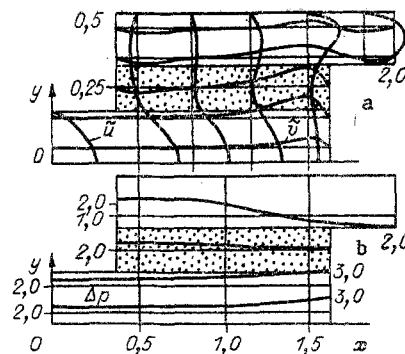


Fig. 3

A substantially nonuniform grid was used in the calculations, and the cells of this grid diminished smoothly on approach to the separation surface G_1 and the walls of the apparatus. Test calculations were conducted on grids 41×21 , 41×31 , 41×41 , and 41×61 . The solutions derived at grids 41×41 and 41×61 coincided and the basic calculations were therefore conducted at the 41×41 grid. At the center of the cell with the checkerboard array we determined the total pressure H , while ω , ψ , u , and v were determined at the nodal points.

The finite-difference equation for ω was solved by the method of a stabilizing correction factor, while the equation for the stream function was solved by the method of upper relaxation. The total-pressure field was found through step-by-step integration of (1.5), (1.6).

Solution for the test problem (the Poiseuille flow and the flow in a channel completely filled with a granular medium) demonstrated that numerical calculation with an accuracy of up to 1% corresponds to the known analytical solution [15].

2. Results of the Calculation. The flow in the apparatus depends on the Reynolds number, the resistance of the granular bed, and the geometric dimensions of the reactor. The regime parameters were varied in these calculations over the following ranges: $Re = 10-200$, $L/D = 1-10$, $d_3/L = 0.04-0.12$, $\epsilon = 0.39-0.78$.

Figure 1 shows the streamlines in the displacement reactor (a) and in the equipment with the Z-shaped fluid flow pattern (b). The computational data were derived for $Re = 75$ and 40 , $\epsilon = 0.39$ and 0.78 , $D = 0.01$ and 0.045 m, $L/D = 8$ and 5 , $d_3/L = 0.07$ and 0.04 (a and b, respectively).

As can be seen from Fig. 1a, the presence of local resistance in the form of the granular bed leads to the dispersion of the fluid to fill the entire cross section of the reactor. The streamlines change little in the granular bed and they collect behind the bed toward the outlet section of the reactor. In the region of pronounced expansion of the chamber and in the streamlining of the corner stagnation zones arise in which the flow of the fluid is reversed. The streamline pattern in the plane reactor with Z-shaped fluid motion is shown in Fig. 1b. The use of viscous-fluid models enables us to detect the presence of stagnation zones in the upper corner of the forward bottom edge of the collector, and these zones include the granular bed. As the resistance of the bed increases, the recirculation zone is shortened and becomes concentrated in the collector, while the streamlines become more uniformly distributed through the length of the NGB.

The velocity and pressure fields shown in Fig. 2 demonstrate the changes in these quantities throughout the entire volume of the displacement reactor. In the case of great permeability on the part of the granular bed, the main portion of the fluid passes through its central portion (the profiles of the longitudinal velocity component $\tilde{u} = \epsilon u$ exhibit a clearly defined jet form with maxima in the plane of symmetry), and with an increase in the resistance of the bed the \tilde{u} profiles straighten out along the length of the granular bed. The transverse velocity component $\tilde{v} = \epsilon v$ in the NGB is small. The lines for the pressure $\Delta p = p - p_0$ in the chamber of the reactor, constructed with respect to the base values, are shown in Fig. 2b. The pressure field changes in accordance with the overall flow pattern, and its drop over the length of the bed follows the Darcy law.

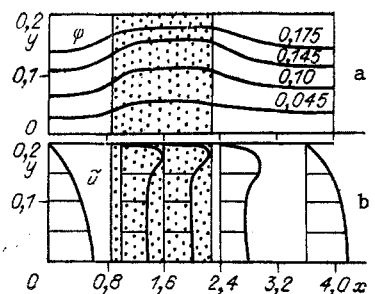


Fig. 4

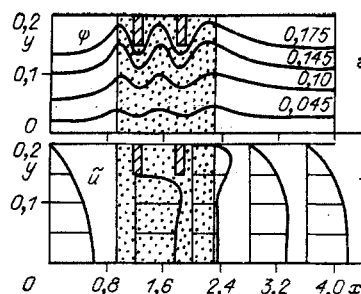


Fig. 5

Figure 3 shows the velocity and pressure fields in a plane apparatus with a Z-shaped flow pattern with the bed in the form of two shells as the fluid drains out symmetrically from the distribution collector. The profiles of the longitudinal velocity component \bar{u} in the supply collector are subjected to continuous deformation and diminish downstream as a consequence of the fluid outflow. It is noteworthy that longitudinal flow reversal occurs within the granular bed, and that there is slippage of the fluid at the free boundaries of the NGB, something that was observed in the experiment conducted in [16]. As the resistance of the bed increases, the \bar{v} profiles become more uniform over the length of the NGB, and there is a corresponding reduction in the longitudinal flow reversal.

There is an increase in the pressure within the flow distributor and a drop in pressure in the flow collector. Such a change in pressure results in nonuniformity in the distribution of the filtration flow along the length of the NGB (Fig. 3b). The calculations showed that with an increase in the length of the NGB and with a reduction in the width of the collecting chamber we are confronted with an increase in the nonuniformity of filtration-flow distribution through the granular bed in an apparatus with Z-shaped flow. In calculation for equipment with symmetrical fluid outflow we observed flow separation from the permeable wall in the final portion of the distribution chamber, owing to the recovery in pressure, which is in agreement with experimental results [17].

In apparatus with a Π -shaped fluid flow pattern the pressure increases within the distribution chamber and drops in the collector, in the direction of the flow. Consequently, the velocity field in the NGB will be more uniform and this pattern is occasionally more preferable from the standpoint of establishing the technological process in comparison to the Z-shaped flow pattern.

We know that an increase in the velocity of the flow in the region near the wall of an apparatus with NGB leads to reduced efficiency in the operating process [18]. Such a phenomenon can be explained by the reduced density of the NGB packing at the walls of the equipment, and this has been confirmed by experimental measurements of porosity [19, 20]. In order to take this effect into consideration, an approximate method was proposed in [21] in which the narrow zone near the wall exhibited a bed porosity of $\varepsilon_w = 0.476$, while the porosity was $\varepsilon = 0.39$ throughout the rest of this section.

Figure 4 shows the results from such a calculation for regime parameters of $Re = 40$, $D = 0.045$ m, $L/D = 5$, $d_3/D = 0.1$. The streamlines bunch up near the wall and the fluid spreads out into the zone of elevated permeability. Consequently, the profiles of the longitudinal velocity component \bar{u} change. Their deformation begins in front of the porous insert, macrononuniformities appear (see Fig. 4b), and these are observed behind the porous insert as well, gradually disappearing downstream. The latter circumstance is explained by the fact that the fluid outflow in the direction of the axis, owing to its deceleration in the boundary bed, intensified vortex formation behind the bed and leads to transformation of the \bar{u} profile prolonged in comparison to the motion of the viscous fluid in the channel through the plane-parallel porous insert [22]. These data are in qualitative agreement with the results familiar from [5, 23, 24].

In actual practice, in order to reduce the effect of porosity nonuniformities at the walls, lateral baffles or rings are mounted on the reactor walls in the region of the granular bed to deflect the flow from the walls, and this leads to more complete filling of the lateral cross section of the reactor. In the calculations for the modeling of these side baffles we introduced segments into the porous bed (the dimensions of these segments matched those of the baffles) with high resistance. As can be seen from Fig. 5, at the points where

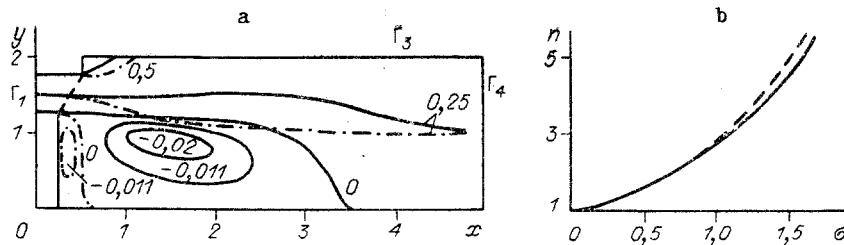


Fig. 6

these baffles are located the streamlines are deflected from the walls and the flow is redistributed and the profiles become more uniform across the segment. No stagnation zones arise in this case and the streamlines smoothly form around the side baffles.

3. Motion Through the Grid. Metallic grids and packets of such grids can be regarded as a thin porous medium. Using the mathematical formulation from [25], we find that the problem reduces to an examination of the following system of equations:

$$\frac{\partial u^2}{\partial x} + \frac{\partial uv}{\partial y} = -\frac{\partial p}{\partial x} + \frac{1}{\text{Re}} \left(\frac{\partial^2 u}{\partial x^2} + \frac{\partial^2 u}{\partial y^2} \right) - \zeta_p u; \quad (3.1)$$

$$\frac{\partial uv}{\partial x} + \frac{\partial v^2}{\partial y} = -\frac{\partial p}{\partial y} + \frac{1}{\text{Re}} \left(\frac{\partial^2 v}{\partial x^2} + \frac{\partial^2 v}{\partial y^2} \right) - \zeta_p v; \quad (3.2)$$

$$\partial u / \partial x + \partial v / \partial y = 0. \quad (3.3)$$

An important characteristic of the influence exerted by the grids on the flow is the refraction of the streamlines [23]. This feature can be studied on the basis of Eqs. (3.1)-(3.3). Let us examine the flow of a viscous fluid in a plane channel with a recess (the geometry is shown in Fig. 6a). Near this recess the channel forms a barrier around the grid, the latter positioned at an angle to the flow. The boundary conditions are as follows: Γ_1 : $u = 1$, $v = 0$, $p = p_0$; Γ_3 : $u = 0$, $v = 0$; Γ_4 : $\partial u / \partial x = 0$, $v = 0$.

The calculations were carried out for given values of the angle θ of flow incidence onto the grid and for grid resistance factors of ζ_p . The refractive properties of the grids were estimated by the extent to which the central streamline was distorted. Figure 6a shows the streamlines for the case in which there is no grid ($\zeta_p = 0$). In the streamlining of the corner, a stagnation zone appears in the area of pronounced channel expansion, with a reverse flow. The calculations carried out with a grid ($\zeta_p = 100$) showed that the streamlines (the dashed-dotted lines) undergo refraction. On the strength of this, in the upper expanded portion of the channel a rarefaction region appears, while the stagnation zone, situated in the lower portion, diminishes sharply and is bounded by a small segment around the streamlined corner.

These calculations were generalized in the form of the function $n = f(\sigma)$ [n is the refractive index of the flow, equal to the ratio of the tangents of the angles of incidence and refraction, $\sigma = \delta a \xi_e / (2\varepsilon)$, where ξ_e is the equivalent coefficient of grid resistance, connected to ζ_p by the relationship $\zeta_p = a D \xi_e / (2\varepsilon^4)$]. Here it is assumed that: $\xi_e = 44.3 / \text{Re}_e$, $\text{Re}_e = u_e d_e / \nu$, $u_e = u / \varepsilon$, $d_e = 4\varepsilon / a$; δ and a are the thickness and specific surface of the grid, respectively.

Figure 6b shows the computational result (the dashed curve), whose comparison with the theoretical function [23] (solid line) indicates their satisfactory agreement within this range of regime parameters.

In conclusion, let us note that the results from the solution of various problems associated with the motion of a viscous fluid in equipment with NGB makes it possible to ascertain numerous quantitative relationships dealing with the aerodynamics of such equipment. From a qualitative standpoint, these are in good agreement with the earlier-known results of theoretical and experimental research.

It seems to us that the developed mathematical model of equipment with NGB can be utilized in approximate engineering calculations.

LITERATURE CITED

1. V. P. Myasniko and V. D. Kotelkin, "The hydrodynamic model of a chemical reactor with a nonmoving catalyst bed," in: Aeromechanics [in Russian], Nauka, Moscow (1976).
2. Yu. P. Esakov and V. D. Kotelkin, "The hydrodynamic model of a reactor with a nonmoving catalyst bed," Dokl. Akad. Nauk SSSR, 289, No. 6 (1986).
3. I. V. Shirko, R. V. Sarkisov, D. N. Motyl', and V. V. Dil'man, "The features of filtration through a porous medium in a chemical reactor with a blocking layer," Teor. Osnovy Khim. Tekh., 20, No. 2 (1986).
4. M. G. Slin'ko and E. V. Badatov, "Hydrodynamic nonuniformities in reactors with a non-moving catalyst bed, and elimination of these nonuniformities," in: Dimensional Transition in Chemical Technology [in Russian], Khimiya, Moscow (1980).
5. M. Yu. Neginskii, "Numerical modeling of fluid and gas flows in porous media," Candidate's Dissertation, Physical-Mathematical Sciences, Moscow (1982).
6. J. Slatterly, The Theory of the Transfer of Momentum, Energy, and Mass, in Continuous Media [Russian translation], Énergiya, Moscow (1978).
7. V. N. Nikolaevskii, The Mechanics of Porous and Fissured Media [in Russian], Nedra, Moscow (1984).
8. H. C. Brinkman, "Calculation of the viscous force exerted by a flowing fluid on a dense swarm of particles," Appl. Sci. Res., A1, No. 1 (1947).
9. A. M. Vaisman and M. A. Gol'dshtik, "The dynamic model of fluid motion in a porous medium," Izv. Akad. Nauk SSSR, Mekh. Zhidk. Gaza, No. 6 (1978).
10. V. A. Mukhin and N. N. Smirnova, "Investigating the processes of heat and mass exchange in the case of filtration in porous media," Preprint No. 26-78, Akad. Nauk SSSR, Sib. Otd., IT, Novosibirsk (1978).
11. C. W. Richards and C. M. Crane, "Pressure marching schemes that work," Int. J. Num. Meth. Eng., 15, No. 4 (1980).
12. L. V. Ovsyannikov, Lectures on the Fundamentals of Gasdynamics [in Russian], Nauka, Moscow (1981).
13. P. Rouch, Computational Hydromechanics [Russian translation], Mir, Moscow (1980).
14. A. A. Samarskii, The Theory of Difference Schemes [in Russian], Nauka, Moscow (1977).
15. B. C. Chandrasekhara, M. Rudraiah, and S. T. Nagaraj, "Velocity and dispersion in porous media," Int. J. Eng. Sci., 18, No. 7 (1980).
16. G. S. Beavers and D. D. Joseph, "Boundary condition at a naturally permeable bed," J. Fluid Mech., 30, No. 1 (1965).
17. J. P. Quaille and E. K. Levy, "Laminar flow in a porous tube with suction," Trans. ASME, Ser. C, J. Heat Trans., 97, No. 1 (1975).
18. M. É. Aéro, O. M. Todes, and D. A. Narinskii, Apparatus with a Steady Granular Bed [in Russian], Khimiya, Leningrad (1979).
19. R. F. Benenati and C. B. Brosilow, "Void fraction distribution in beds of spheres," AIChE J., 8, No. 3 (1962).
20. Yu. A. Buyevich, V. M. Korolyov, and N. I. Syromyatnikov, "Hydrodynamic conditions for the external heat exchange in granular beds," in: 16th JCHMT Int. Symp. Heat and Mass Trans. in Fixed and Fluid Beds, Dubrovnik, Yugoslavia (1984); Preprint of Report.
21. N. M. Zhavoronkov, M. É. Aéro, and N. I. Umnik, "Hydraulic resistance and the density of packing for the granular layer," Zh. Fiz. Khim., 23, No. 3 (1949).
22. N. T. Danaev, Sh. A. Ershin, U. K. Zhabbasbaev, and M. Sh. Kulymbaeva, "Numerical investigation into the motion of a viscous incompressible fluid in channels with a permeable barrier," Vestn. Akad. Nauk KazSSR, No. 10 (1987).
23. M. A. Gol'dshtik, The Processes of Transport in a Granular Bed [in Russian], IT SO Akad. Nauk SSSR, Novosibirsk (1984).
24. I. V. Shirko, "Numerical investigation of flows in granular layers," in: Numerical Modeling in Aerodynamics [in Russian], Nauka, Moscow (1986).
25. V. A. Marchenko and E. Ya. Khruslov, Boundary-Value Problems in a Region with a Small-Grain Boundary [in Russian], Naukova Dumka, Kiev (1974).